Research Article

A Forward-Backward Kalman Filter-based STBC MIMO OFDM Receiver

T. Y. Al-Naffouri and A. A. Quadeer

Electrical Engineering Department, King Fahd University of Petroleum and Minerals, Dhahran 31261, Saudi Arabia

Correspondence should be addressed to A. A. Quadeer, aquadeer@kfupm.edu.sa

Orthogonal frequency division multiplexing (OFDM) has emerged as a modulation scheme that can achieve high data rates over frequency selective fading channel by efficiently handling multipath effects. This paper proposes receiver design for space-time block coded MIMO OFDM transmission over frequency selective time-variant channels. Joint channel and data recovery are performed at the receiver by utilizing the expectation-maximization (EM) algorithm. It makes collective use of the data constraints (pilots, cyclic prefix, the finite alphabet constraint, and space-time block coding) and channel constraints (finite delay spread, frequency and time correlation, and transmit and receive correlation) to implement an effective receiver. The channel estimation part of the receiver boils down to an EM-based forward-backward Kalman filter. A forward-only Kalman filter is also proposed to avoid the latency involved in estimation. Simulation results show that the proposed receiver outperforms other least-squares-based iterative receivers.

1. INTRODUCTION

Orthogonal frequency division multiplexing (OFDM) is a technique that enables high speed transmission over frequency selective channels with simple equalizers. It does this by creating a set of parallel frequency-flat channels over which large constellation signals can be transmitted. For frequency flat fading channels, space-time codes provide diversity and coding gain benefits compared with single-input single-output (SISO) systems improving the BER performance of the system [1]. (We concentrate in this work on space-frequency codes. We note however that a very similar approach can be used for space-time block codes (STBC). Given the similarity between the two approaches and the fact that the abbreviation STBC is more familiar, we continue to use this abbreviation to refer to our frequency-space codes.) When multiple antennas (MIMO) are combined with OFDM, space-time codes can be used per tone, providing the benefit of multiple antennas with simple channel equalization.

An OFDM receiver needs channel state information (CSI) to detect the data. With no CSI at the receiver, both the channel and the data are unknowns that have to be recovered. The estimation process can be carried out jointly or separately. Techniques for channel estimation fall into 3 distinct classes: (1) training/pilot-based, (2) semiblind, and (3) blind methods. Training/pilot-based methods estimate the channel from a known preamble/pilot sequence sent at the transmitter and use the estimated channel to decode the data [2–7]. Blind methods do not use any preambles/pilots but rely instead on *a priori* constraints to recover the channel and data. The data constraints include redundancy due to the cyclic prefix [8, 9], nonredundant, and nonconstant-modulus precoding [10], constant-modulus modulation [11], subspace-based constraints [12], and the finite alphabet constraint [13]. Semiblind methods make use of both pilots and additional channel/input data constraints to perform channel identification and equalization. These methods use pilots to obtain an initial channel estimate and improve the estimate by using a variety of *a priori* information. Thus, in addition to the aforementioned constraints, semiblind methods use the time and frequency correlation [14] and the subspace of the channel [15]. The channel estimate can also be improved iteratively in a data-aided fashion [12], or more rigorously by the expectation maximization (EM) approach [16–21].

1.1. Paper contributions

This paper considers receiver design for OSTBC-OFDM transmission over a frequency selective, time-variant channel. We propose a semiblind iterative receiver using the EM algorithm for joint channel and data recovery. The main contributions of the work are summarized below.

(1) We make a collective use of the structure of the communication problem (i.e., the constraints on the data and on the channel) in a transparent manner. The data constraints include the finite alphabet constraint [13], the cyclic prefix [8], pilots [6, 7], and the OSTBC. In addition, the receiver uses the following constraints on the channel: the finite delay spread, frequency and time correlation [22–24], and spatial correlation (it is also straightforward to incorporate channel sparsity [15, 25, 26]). This is in contrast to the work done by other researchers as none has used all the above mentioned constraints in such a collective and transparent manner.

(2) The channel estimation and data detection as well as the exploitation of the system constraints is done in a semioptimal manner through the EM algorithm. This guarantees a simple receiver structure.

(3) In spite of the complexity of the problem that we address here and the many constraints we incorporate, our algorithm maintains its transparency:

  (a) the maximization step is used for channel estimation and makes use of the channel constraints by employing a forward-backward Kalman filter.

  (b) the expectation step is used for data detection and makes use of the data constraints.

(4) In contrast to prior approaches, we take a channel estimation centric viewpoint and reverse the roles of the channel and the transmitted signal in our implementation of the EM algorithm [19] using the estimation step for data detection and maximization step for channel estimation. We do so because it is difficult to employ the expectation step for channel estimation while simultaneously incorporating the various constraints on the channel (most notably, the time-correlation constraint).

A similar algorithm was proposed by the first author in [27] for the SISO case. Extending this algorithm to the MIMO case is nontrivial. For in addition to the scale up in the number of transmit and receive antennas, this paper (1) makes use of the space-time code and (2) makes full use of the frequency and time correlation as well as transmit and receive spatial correlation (see Section 2.2 and Appendix A where we derive the channel model). Moreover, and in spite of the many dimensions we deal with, we maintain the transparency of the presentation.

1.2. Paper organization

The paper is organized as follows. After introducing our notation, we give an overview of the transceiver in Section 2. Section 3 then derives the input/output (I/O) equations for MIMO-OFDM with ST coding (the equations are needed for channel and data recovery). Channel estimation using the forward-backward (FB) Kalman filter is derived in Section 4 at the end of which we summarize the transceiver algorithm with an extension/modification of the algorithm. Section 5 presents our simulations and Section 6 presents our conclusions.

1.3. Notation

Proper choice of notation is essential for clarity and consistency. One challenge in choosing notation is the many dimensions we deal with in this paper including sample time, (frequency) tone, (channel) tap, (OFDM) symbol index, and space.

In this paper, we denote scalars with small-case letters (e.g., x), vectors with small-case boldface letters (e.g., $\mathbf{x}$), and matrices with uppercase boldface letters (e.g., $\mathbf{X}$). Calligraphic notation (e.g., $\mathcal{X}$) is reserved for vectors in the frequency domain. A hat over a variable indicates an estimate of the variable (e.g., $\hat{\mathbf{h}}$ is an estimate of $\mathbf{h}$). We use $*$ to denote conjugate transpose, $\otimes$ to denote Kronecker product, $\mathbf{I}_N$ to denote the size $N \times N$ identity matrix, and $\mathbf{0}_{M \times N}$ to denote the all zero $M \times N$ matrix. Given a sequence of vectors $\mathbf{h}_{r_x}^{t_x}$ for $r_x = 1 \cdots R_x$ and $t_x = 1 \cdots T_x$, we define the following stack variables:

$$\mathbf{h}_{r_x} = \begin{bmatrix} \mathbf{h}_{r_x}^1 \\ \vdots \\ \mathbf{h}_{r_x}^{T_x} \end{bmatrix}, \qquad \mathbf{h} = \begin{bmatrix} \mathbf{h}_1 \\ \vdots \\ \mathbf{h}_{R_x} \end{bmatrix}. \tag{1}$$

The notation vec($\mathbf{X}$) denotes a column vector consisting of the concatenation of all column vectors of $\mathbf{X}$ while the operation diag($\mathcal{X}$) transforms the vector $\mathcal{X}$ into a matrix with diagonal $\mathcal{X}$.

2. AN OVERVIEW OF THE COMMUNICATION SYSTEM

In this section, we give an overview of the communications system: transmitter, channel, and receiver.

2.1. Transmitter

A block diagram of the transmitter is shown in Figure 1. The bit sequence to be transmitted passes through a convolutional encoder that serves as an outer code for the system. The coded output is punctured to increase the code rate. The punctured sequence then passes through a random interleaver which rearranges the order of the bits according to a random permutation. The interleaved bit sequence is mapped to QAM symbols (or any modulation scheme for that matter) using Gray coding and the QAM symbols are in turn mapped to the OFDM symbols with some tones reserved for the pilot symbols. The STBC encoder uses the OFDM
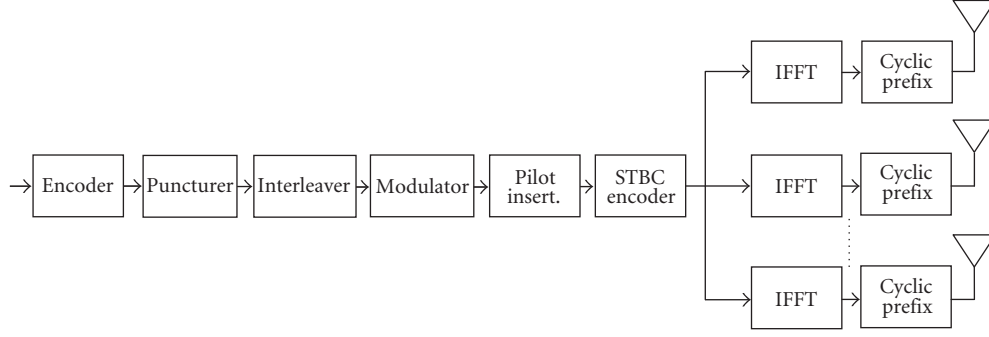
FIGURE 1: OSTBC OFDM transmitter.

symbols to construct the ST block by mapping the various OFDM symbols to a specific antenna and specific time slot depending on the ST code used. Each antenna performs an IFFT operation on the OFDM symbols to produce the time-domain OFDM symbols and adds a cyclic prefix to each prior to transmission.

2.2. Channel model

We consider a time-variant and frequency selective MIMO channel. For a general MIMO system, the I/O time-domain relationship is described by

$$\mathbf{y}(m) = \sum_{p=0}^{P} \mathbf{H}(p)\mathbf{x}(m-p), \qquad (2)$$

where $\mathbf{H}(p)$ is the $R_x \times T_x$ MIMO impulse response at tap p and where m represents the sample time index. The taps $\mathbf{H}(p)$ usually incorporate the effect of the transmit filter and the effects of the transmit and receive correlation making $\mathbf{H}(p)$ correlated across space and tap. We will assume for simplicity that $\mathbf{H}(p)$ is iid for all p (In Appendix A we consider the general case where the channel exhibits transmit and receive correlation). We will also assume that the tap $\mathbf{H}(p)$ remains constant over a single ST block (and hence over the constituent OFDM symbols) and changes from the current block ($\mathbf{H}_t(p)$) to the next ($\mathbf{H}_{t+1}(p)$) according to the dynamical equation (We will at times suppress the time dependence for notational convenience.)

$$\mathbf{H}_{t+1}(p) = \alpha(p)\mathbf{H}_t(p) + \sqrt{(1-\alpha^2(p))e^{-\beta p}}\,\mathbf{U}_t(p). \quad (3)$$

Here, $\mathbf{U}_t(p)$ is an iid matrix with entries that are $N(0,1)$, and $\alpha(p)$ is related to the Doppler frequency $f_D(p)$ by $\alpha(p) = J_0(2\pi f_D(p)T)$, where T is the time duration of one ST block. The variable β in (3) corresponds to the exponent of the channel decay profile while the factor $\sqrt{(1-\alpha^2(p))e^{-\beta p}}$ ensures that each link maintains the exponential decay profile ($e^{-\beta p}$) for all time.

This channel model allows the channel to be time variant (as the channel can change arbitrarily from one ST block to the next) while avoiding intercarrier interference and ensuring the proper operation of the space-time code (as the channel remains fixed over any one OFDM symbol or

ST block). This model was adopted in [23, 28, 29] in an SISO context. (This model is based on approximating the nonrational Jakes model by a first-order AR model. It is also possible to have a better approximation by employing higher-order AR models but this would increase the latency of the receiver.)

In this paper, we scale up the model to the MIMO case and also show how to incorporate transmit and receive correlation in Appendix A (see [27, 30] where we also incorporate the effect of the receive filter).

Using this dynamical model, we can obtain the state-space model for the impulse response $\mathbf{h}_{r_x}^{t_x}$ between transmit antenna t_x and receive antenna r_x. From (3), we can write

$$h_{r_x,t+1}^{t_x}(p) = \alpha(p)h_{r_x,t}^{t_x}(p) + \sqrt{(1-\alpha^2(p))e^{-\beta p}}\,u_{r_x,t}^{t_x}(p). \quad (4)$$

By stacking (4) over the taps $p = 0, 1, \ldots, P$, we obtain the dynamical model

$$\mathbf{h}_{r_x,t+1}^{t_x} = \mathbf{F}\mathbf{h}_{r_x,t}^{t_x} + \mathbf{G}\mathbf{u}_{r_x,t}^{t_x}, \qquad (5)$$

where

$$\mathbf{F} = \begin{bmatrix} \alpha(0) & & \\ & \ddots & \\ & & \alpha(P) \end{bmatrix},$$

$$\mathbf{G} = \begin{bmatrix} \sqrt{1-\alpha^2(0)} & & \\ & \ddots & \\ & & \sqrt{(1-\alpha^2(P))e^{-\beta P}} \end{bmatrix}. \qquad (6)$$

By further stacking (5) over all transmit and receive antennas (refer to our stacking notation in (1)), we obtain

$$\mathbf{h}_{t+1} = (\mathbf{I}_{T_x R_x} \otimes \mathbf{F})\mathbf{h}_t + (\mathbf{I}_{T_x R_x} \otimes \mathbf{G})\mathbf{u}_t, \qquad (7)$$

where $\mathbf{h}_{t+1}, \mathbf{h}_t$, and $\mathbf{u}_t$, are vectors of size $T_x R_x(P+1) \times 1$. The dynamical equation (7) shows explicit dependence on the space-time index t (so $t = 1$ for the first space-time symbol which consists of two OFDM symbols in the Alamouti case, $t = 2$ for the second space-time symbol, etc.).

For complete characterization of the dynamical model, we need to specify the covariance of $\mathbf{u}_t$, and also the

covariance of the channel at the first time instant. It is easy to show that

$$E[\mathbf{u}_t\mathbf{u}_t^*] = \mathbf{I}_{R_x} \otimes E[\mathbf{u}_{r_x}\mathbf{u}_{r_x}^*]$$
$$= \mathbf{I}_{R_x} \otimes (\mathbf{I}_{T_x} \otimes E[u_{r_x}^{t_x}u_{r_x}^{t_x*}]) \qquad (8)$$
$$= \mathbf{I}_{R_x} \otimes \mathbf{I}_{T_x} \otimes \mathbf{I}_{P+1} = \mathbf{I}_{T_xR_x(P+1)}.$$

We can similarly show that the channel covariance at the first time instant is given by

$$E[\mathbf{h}_0\mathbf{h}_0^*] = \mathbf{I}_{T_xR_x} \otimes \mathbf{GG}^*. \qquad (9)$$

The covariance information is important for employing the Kalman filter which is used for channel estimation. We finally note that while (3) and (7) are equivalent, the latter model is in vector form and hence lends itself more to the Kalman filter operations, which are used for channel estimation.

A note about time variation

One drawback of the approach in this paper is the block fading model that we adopt. For it is more realistic to assume that the channel continuously varies with time. There are 3 justifications for using the block fading model.

(1) While it is more realistic to assume that the channel continuously varies over the OFDM symbol, the model we assume is more valid than the block-fading model that is widely used in literature. For in the block-fading model, it is usually assumed that the channel remains constant over any one symbol and varies *independently* from one symbol to another. Here, we account for the time correlation across symbols.

(2) The purpose of this paper is to design an algorithm that makes a collective use of the underlying structure of the communication problem to lower the training overhead required in the time-variant case. Solving the general time-variant case is a future research problem that builds upon the findings in this paper [31].

(3) One could still envision applications where the channel is constant over an ST block, but varies substantially from one symbol to the next. Consider, for example, a multiuser application in which the wireless channel is time shared. Imagine also that the channel is very slowly time variant but the duty cycle is very large. In that case, the channel that each user experiences during his transmission burst is very slow, but from one burst to another, the channel would change substantially due to the long duty cycle. This situation would also make sense in random access scenarios.

2.3. Receiver

This paper is concerned with designing a receiver for the system described above. For completeness and as an allusion to the developments further ahead, Figure 2 shows a block diagram of the proposed receiver. As we will show, the receiver's core operation is based on the EM algorithm which performs joint channel and data recovery.

2.3.1. STBC *decoder/data detector (estimation step)*

The STBC decoder/data detector calculates the conditional first and second moments of the transmitted data (soft estimate) to be used by the channel estimator.

2.3.2. *channel estimator (maximization step)*

Pilots are used to initialize channel estimation. The channel estimator then uses the soft data estimates together with the data and channel constraints to improve the channel estimate. These two processes (channel estimation and data detection) go on iteratively until a stopping criterion is satisfied.

3. INPUT/OUTPUT EQUATIONS FOR MIMO-OFDM

As pointed out in Section 2.3, the receiver performs two operations, channel estimation and data detection. As such, we need to derive two forms of the I/O equations: one that lends itself to *channel estimation* (i.e., treats the channel impulse response as the unknown) and a dual version that lends itself to *data detection* (i.e., treats the input in its uncoded form as the unknown). To this end, let $\mathcal{X}_{t_x}$ be the OFDM symbol transmitted through antenna t_x which first undergoes an IDFT $\mathbf{x}_{t_x} = 1/N\mathbf{Q}\mathcal{X}_{t_x}$ where $\mathbf{Q}$ is the $N \times N$ IDFT matrix. The system then appends a cyclic prefix before transmission. At the receiver end, the receiver strips the cyclic prefix to obtain the time domain symbol $\mathbf{y}_{r_x}^{t_x}$. The I/O equation of the OFDM system between transmit antenna t_x and receive antenna r_x is best described in the frequency domain

$$\mathcal{Y}_{r_x}^{t_x} = \mathrm{diag}(\mathcal{X}_{t_x})\mathbf{Q}_{P+1}^*\mathbf{h}_{r_x}^{t_x} + \mathcal{N}_{r_x}, \qquad (10)$$

where $\mathcal{Y}_{r_x}^{t_x}, \mathcal{X}_{t_x}, \mathcal{H}_{r_x}^{t_x}$, and $\mathcal{N}_{r_x}^{t_x}$ are the (length-N) DFTs of $\mathbf{y}_{r_x}^{t_x}, \mathbf{x}_{t_x}, \mathbf{h}_{r_x}^{t_x}, \mathbf{n}_{r_x}$, respectively, and where (10) follows from the fact that

$$\mathcal{H}_{r_x}^{t_x} = \mathbf{Q}^* \begin{bmatrix} \mathbf{h}_{r_x}^{t_x} \\ \mathbf{O}_{(N-P-1)\times 1} \end{bmatrix} = \mathbf{Q}_{P+1}^*\mathbf{h}_{r_x}^{t_x}. \qquad (11)$$

Here, $\mathbf{Q}_{P+1}$ represents the first $P + 1$ rows of $\mathbf{Q}$. By superposition and using the stacking notation (1), we can express the I/O equation at receive antenna r_x as

$$\mathcal{Y}_{r_x} = [\mathrm{diag}(\mathcal{X}_1) \cdots \mathrm{diag}(\mathcal{X}_{T_x})](\mathbf{I}_{T_x} \otimes \mathbf{Q}_{P+1}^*)\mathbf{h}_{r_x} + \mathcal{N}_{r_x}. \qquad (12)$$

3.1. I/O *equations: channel estimation version*

Consider a set of N_u uncoded OFDM symbols $\{\mathcal{S}(1),\dots,\mathcal{S}(N_u)\}$ which we would like to transmit over T_x antennas and N_c time slots. Following [32], we can perform ST coding using the set of $T_x \times N_c$ matrices $\{\mathbf{A}(1),\mathbf{B}(1),\dots,\mathbf{A}(N_u),\mathbf{B}(N_u)\}$ which characterizes the ST code. We can now show that the OFDM symbol transmitted from antenna t_x at time n_c is given by [32]:

$$\mathcal{X}_{t_x}(n_c) = \sum_{n_u=1}^{N_u} a_{t_x,n_c}(n_u)\mathrm{Re}\,\mathcal{S}(n_u) + jb_{t_x,n_c}(n_u)\mathrm{Im}\,\mathcal{S}(n_u),$$
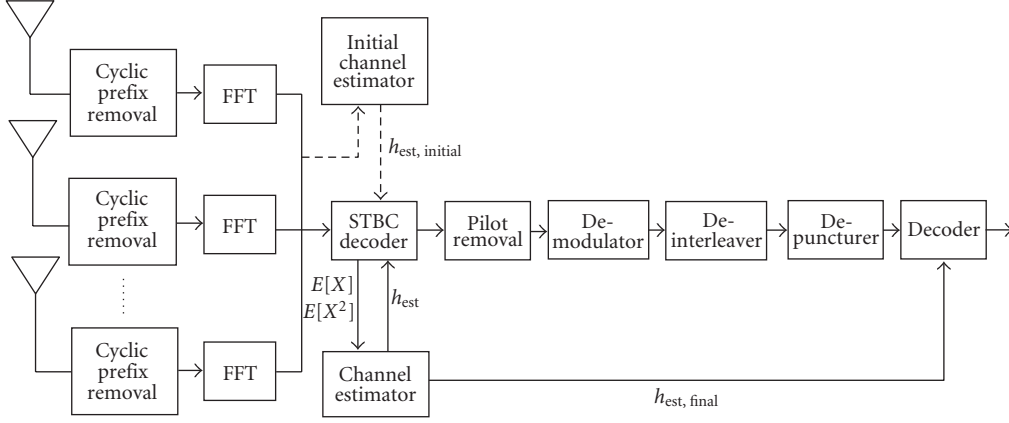
$$(13)$$

FIGURE 2: OSTBC OFDM receiver.

where $a_{t_x,n_c}(n_u)$ is the (t_x, n_c) element of $\mathbf{A}(n_u)$ and $b_{t_x,n_c}(n_u)$ is the (t_x, n_c) element of $\mathbf{B}(n_u)$. Thus, in the presence of ST coding, (12) reads

$$
\boldsymbol{\mathcal{Y}}_{r_x}(n_c) = [\mathrm{diag}(\boldsymbol{\mathcal{X}}_1(n_c)) \cdots \mathrm{diag}(\boldsymbol{\mathcal{X}}_{T_x}(n_c))] \\
\times (\mathbf{I}_{T_x} \otimes \mathbf{Q}_{P+1}^*)\mathbf{h}_{r_x} + \boldsymbol{\mathcal{N}}_{r_x}(n_c). \tag{14}
$$

(It should be clear that by using an ST code, a diversity of $T_x \times R_x$ is achieved by spreading each symbol in time and space at the transmitter antenna. The symbols are not spread in frequency and thus, (multipath) diversity is lost at the price of decoding simplicity (i.e., bin by bin decoupling).) This represents the I/O equation at antenna r_x at OFDM symbol n_c of an ST block. Collecting this equation for all such symbols yields

$$
\boldsymbol{\mathcal{Y}}_{r_x} = \mathbf{X}\mathbf{h}_{r_x} + \boldsymbol{\mathcal{N}}_{r_x}, \tag{15}
$$

where

$$
\boldsymbol{\mathcal{Y}}_{r_x} = \begin{bmatrix} \boldsymbol{\mathcal{Y}}_{r_x}(1) \\ \vdots \\ \boldsymbol{\mathcal{Y}}_{r_x}(N_c) \end{bmatrix},
$$

$$
\mathbf{X} = \begin{bmatrix} \{\mathrm{diag}(\boldsymbol{\mathcal{X}}_1(1)) \cdots \mathrm{diag}(\boldsymbol{\mathcal{X}}_{T_x}(1))\}(\mathbf{I}_{T_x} \otimes \mathbf{Q}_{P+1}^*) \\ \{\mathrm{diag}(\boldsymbol{\mathcal{X}}_1(2)) \cdots \mathrm{diag}(\boldsymbol{\mathcal{X}}_{T_x}(2))\}(\mathbf{I}_{T_x} \otimes \mathbf{Q}_{P+1}^*) \\ \vdots \\ \{\mathrm{diag}(\boldsymbol{\mathcal{X}}_1(N_c)) \cdots \mathrm{diag}(\boldsymbol{\mathcal{X}}_{T_x}(N_c))\}(\mathbf{I}_{T_x} \otimes \mathbf{Q}_{P+1}^*) \end{bmatrix}. \tag{16}
$$

Now, by further collecting this relationship over all receive antennas, we obtain

$$
\boldsymbol{\mathcal{Y}}_t = (\mathbf{I}_{R_x} \otimes \mathbf{X}_t)\mathbf{h}_t + \boldsymbol{\mathcal{N}}_t. \tag{17}
$$

This equation captures the I/O relationship at *all* frequency bins, for *all* input and output antennas, and for *all* OFDM symbols of the tth ST block.

To perform initial channel estimation, we select those equations where the pilots are present. Let I_p denote the index set of the pilots bins. Then, the pilot/output equation takes the form

$$
\boldsymbol{\mathcal{Y}}_{t_{I_p}} = (\mathbf{I}_{R_x} \otimes \mathbf{X}_{t_{I_p}})\mathbf{h}_t + \boldsymbol{\mathcal{N}}_{t_{I_p}}. \tag{18}
$$

As can be seen, (17) and (18) are quite similar and using them in a Kalman filter context will be similar as well.

3.2. I/O *equations: data detection version*

Signal detection in ST-coded OFDM is done on a tone-by-tone basis (as in SISO OFDM), except that the tones are collected for the whole ST block (i.e., for R_x receive antennas and over N_c time slots). From (10), we can construct the following I/O equation *at any tone n* belonging to the OFDM symbol n_c:

$$
\boldsymbol{\mathcal{Y}}_{r_x}(n_c) = \begin{bmatrix} \boldsymbol{\mathcal{H}}_{r_x}^1 & \cdots & \boldsymbol{\mathcal{H}}_{r_x}^{T_x} \end{bmatrix} \begin{bmatrix} \boldsymbol{\mathcal{X}}_1(n_c) \\ \vdots \\ \boldsymbol{\mathcal{X}}_{T_x}(n_c) \end{bmatrix} + \boldsymbol{\mathcal{N}}_{r_x}(n_c). \tag{19}
$$

We suppress the dependence on n for notational convenience. Collecting this relationship for all receive antennas yields

$$
\begin{bmatrix} \boldsymbol{\mathcal{Y}}_1(n_c) \\ \vdots \\ \boldsymbol{\mathcal{Y}}_{R_x}(n_c) \end{bmatrix} = \begin{bmatrix} \boldsymbol{\mathcal{H}}_1^1 & \cdots & \boldsymbol{\mathcal{H}}_1^{T_x} \\ \vdots & \cdots & \vdots \\ \boldsymbol{\mathcal{H}}_{R_x}^1 & \cdots & \boldsymbol{\mathcal{H}}_{R_x}^{T_x} \end{bmatrix} \begin{bmatrix} \boldsymbol{\mathcal{X}}_1(n_c) \\ \vdots \\ \boldsymbol{\mathcal{X}}_{T_x}(n_c) \end{bmatrix} + \begin{bmatrix} \boldsymbol{\mathcal{N}}_1(n_c) \\ \vdots \\ \boldsymbol{\mathcal{N}}_{R_x}(n_c) \end{bmatrix}, \tag{20}
$$

or, more succinctly,

$$
\boldsymbol{\mathcal{Y}}(n_c) = \mathbf{H}\boldsymbol{\mathcal{X}}(n_c) + \boldsymbol{\mathcal{N}}(n_c). \tag{21}
$$

By further concatenating this relationship for $n_c = 1, \ldots, N_c$, we can show that the following relationship holds (see [32]):

$$
\boldsymbol{\mathcal{Y}} = \mathbf{C}\begin{bmatrix} \mathrm{Re}\,\boldsymbol{\mathscr{S}} \\ \mathrm{Im}\,\boldsymbol{\mathscr{S}} \end{bmatrix} + \boldsymbol{\mathcal{N}}, \tag{22}
$$

where

$$
\boldsymbol{\mathcal{Y}} = \begin{bmatrix} \boldsymbol{\mathcal{Y}}(1) \\ \vdots \\ \boldsymbol{\mathcal{Y}}(N_c) \end{bmatrix}, \qquad \boldsymbol{\mathscr{S}} = \begin{bmatrix} \boldsymbol{\mathscr{S}}(1) \\ \vdots \\ \boldsymbol{\mathscr{S}}(N_u) \end{bmatrix}, \qquad \mathbf{C} = \begin{bmatrix} \mathbf{C}_a & \mathbf{C}_b \end{bmatrix}, \tag{23}
$$

with $\mathbf{C}_a = [\ \text{vec}(\mathbf{HA}(1))\ \cdots\ \text{vec}(\mathbf{HA}(N_u))\ ]$ and $\mathbf{C}_b = [\ \text{vec}(\mathbf{HB}(1))\ \cdots\ \text{vec}(\mathbf{HB}(N_u))\ ]$. We finally note that the STBC code is orthogonal if and only if the matrix $\mathbf{C}$ satisfies [32]

$$\text{Re}[\mathbf{C}^*\mathbf{C}] = \|\mathbf{H}\|^2 \mathbf{I}_{2N_u} \quad \forall \mathbf{H}. \tag{24}$$

This property is essential to perform data detection. We stress that the relationships (19) through (24) apply at a particular tone n and that this dependence has been omitted for notational convenience.

4. JOINT CHANNEL AND DATA ESTIMATION: AN EM APPROACH

4.1. The EM algorithm

Consider the I/O equation (17) reproduced here for convenience

$$\boldsymbol{\mathcal{Y}}_t = (\mathbf{I}_{R_x} \otimes \mathbf{X}_t)\mathbf{h}_t + \boldsymbol{\mathcal{N}}_t. \tag{25}$$

Ideally, we estimate $\mathbf{h}_t$ by maximizing some log-likelihood function, for example,

$$\hat{\mathbf{h}}_t^{\text{MAP}} = \max_{\mathbf{h}_t} \ln p(\boldsymbol{\mathcal{Y}}_t \mid \mathbf{X}_t, \mathbf{h}_t) + \ln p(\mathbf{h}_t). \tag{26}$$

In our case, however, the input $\mathbf{X}_t$ is not available. Thus, we use the EM algorithm and maximize instead an averaged form of the log-likelihood function. Specifically, starting from an initial estimate $\hat{\mathbf{h}}_t^{(0)}$, the estimate $\hat{\mathbf{h}}_t$ is calculated iteratively, with the estimate at the jth iteration given by

$$\hat{\mathbf{h}}_t^{(j)} = \arg\max_{\mathbf{h}_t} E_{X_t \mid \boldsymbol{\mathcal{Y}}_t, \hat{h}_t^{(j-1)}} \ln p(\boldsymbol{\mathcal{Y}}_t \mid \mathbf{X}_t, \mathbf{h}_t) + \ln p(\mathbf{h}_t). \tag{27}$$

For example, when the system obeys the I/O relationship (25) and $\mathbf{h}_t$ is $\mathcal{N}(\mathbf{0}, \mathbf{\Pi})$, the EM-based estimate (at the jth iteration) is given by

$$\hat{\mathbf{h}}_t^{(j)} = \arg\min_{\mathbf{h}_t} \|\boldsymbol{\mathcal{Y}}_t - (\mathbf{I}_{R_x} \otimes E[\mathbf{X}_t])\mathbf{h}_t\|^2_{1/\sigma_n^2} + \|\mathbf{h}_t\|^2_{I \otimes \text{Cov}[\mathbf{X}_t^*]} + \|\mathbf{h}_t\|^2_{\mathbf{\Pi}^{-1}}, \tag{28}$$

where the two moments of $\mathbf{X}_t$ are taken given the output $\boldsymbol{\mathcal{Y}}_t$ and the most recent channel estimate $\mathbf{h}_t^{(j-1)}$. (The weighted norm notation $\|\mathbf{h}\|_A^2$ stands for $\mathbf{h}^*A\mathbf{h}$.) We now derive the EM algorithm for the time-variant case.

4.2. Channel estimation: an EM-based forward-backward Kalman

Consider the OFDM system of this paper, essentially described by the state-space model

$$\mathbf{h}_{t+1} = (\mathbf{I}_{T_x R_x} \otimes \mathbf{F})\mathbf{h}_t + (\mathbf{I}_{T_x R_x} \otimes \mathbf{G})\mathbf{u}_t, \tag{29}$$

$$\boldsymbol{\mathcal{Y}}_t = (\mathbf{I}_{R_x} \otimes \mathbf{X}_t)\mathbf{h}_t + \boldsymbol{\mathcal{N}}_t, \tag{30}$$

with $\mathbf{h}_0 \sim \mathcal{N}(\mathbf{0}, \mathbf{\Pi})$ and $\mathbf{u}_t \sim \mathcal{N}(\mathbf{0}, \mathbf{R}_u)$. Given a sequence of $T+1$ input and output ST symbols $\mathbf{X}_0^T$ and $\boldsymbol{\mathcal{Y}}_0^T$, (we use

$\mathbf{X}_0^T$ to denote the sequence $\mathbf{X}_0, \mathbf{X}_1, \ldots, \mathbf{X}_T$) we obtain the MAP estimate of the channel sequence $\mathbf{h}_0^T$ by maximizing the log-likelihood

$$\mathcal{L} = \ln p(\boldsymbol{\mathcal{Y}}_0^T \mid \mathbf{X}_0^T, \mathbf{h}_0^T) + \ln p(\mathbf{h}_0^T). \tag{31}$$

Now, using (30), we can express the first term of the log-likelihood (up to some additive constant) as

$$\ln p(\boldsymbol{\mathcal{Y}}_0^T \mid \mathbf{X}_0^T, \mathbf{h}_0^T) = \sum_{t=0}^{T} \ln p(\boldsymbol{\mathcal{Y}}_t \mid \boldsymbol{\mathcal{X}}_t, \mathbf{h}_t)$$
$$= -\sum_{t=0}^{T} \|\boldsymbol{\mathcal{Y}}_t - (\mathbf{I}_{R_x} \otimes \mathbf{X}_t)\mathbf{h}_t\|^2_{1/\sigma_n^2}. \tag{32}$$

Similarly, using (29), we can express the second term of (31) (again up to some additive constant) as

$$\ln p(\mathbf{h}_0^T) = \sum_{t=1}^{T} \ln p(\mathbf{h}_t \mid \mathbf{h}_{t-1}) + \ln p(\mathbf{h}_0)$$
$$= -\sum_{t=1}^{T} \|\mathbf{h}_t - (\mathbf{I}_{T_x R_x} \otimes \mathbf{F})\mathbf{h}_{t-1}\|^2_{(GR_u G^*)^{-1}} - \|\mathbf{h}_0\|^2_{\mathbf{\Pi}_0^{-1}}. \tag{33}$$

Combining these two expressions yields

$$\mathcal{L} = -\sum_{t=1}^{T} \|\boldsymbol{\mathcal{Y}}_t - (\mathbf{I}_{R_x} \otimes \mathbf{X}_t)\mathbf{h}_t\|^2_{1/\sigma_n^2}$$
$$- \sum_{t=1}^{T} \|\mathbf{h}_t - (\mathbf{I}_{T_x R_x} \otimes \mathbf{F})\mathbf{h}_{t-1}\|^2_{(GR_u G^*)^{-1}} - \|\mathbf{h}_0\|^2_{\mathbf{\Pi}_0^{-1}}. \tag{34}$$

Since the channel sequence $\mathbf{h}_0^T$ is jointly Gaussian, the MAP estimate of the channel sequence given the input and output sequences $\mathbf{X}_0^T$ and $\boldsymbol{\mathcal{Y}}_0^T$ is the same as the MMSE estimate given the same sequences. The MMSE estimate itself is obtained by the forward-backward (FB) Kalman filter. This allows us to state the following theorem. (For a proof, see [33, problem 10.9].)

Theorem 1 (channel estimation-known input case). *Consider the state-space model (29)-(30). Given the input and output sequences $\mathbf{X}_0^T$ and $\boldsymbol{\mathcal{Y}}_0^T$, the MAP (or equivalently MMSE) estimate of $\mathbf{h}_0^T$ is obtained by applying the following (forward-backward Kalman) filter to the state-space model (29)-(30).*

Forward run

For $i = 1, \ldots, T$, calculate

$$\mathbf{R}_{e,t} = \sigma_n^2 \mathbf{I}_{T_x R_x N} + (\mathbf{I}_{R_x} \otimes \mathbf{X}_t)\mathbf{P}_{t|t-1}(\mathbf{I}_{R_x} \otimes \mathbf{X}_t^*) \quad \mathbf{P}_{0|-1} = \mathbf{\Pi}_0, \tag{35}$$

$$\mathbf{K}_t = \mathbf{P}_{t|t-1}(\mathbf{I}_{R_x} \otimes \mathbf{X}_t^*)\mathbf{R}_{e,t}^{-1}, \tag{36}$$

$$\hat{\mathbf{h}}_{t|t} = (\mathbf{I}_{T_x R_x(P+1)} - \mathbf{K}_t(\mathbf{I}_{R_x} \otimes \mathbf{X}_t))\hat{\mathbf{h}}_{t|t-1} + \mathbf{K}_t \boldsymbol{\mathcal{Y}}_t, \tag{37}$$

$$\hat{\mathbf{h}}_{t+1|t} = (\mathbf{I}_{T_x R_x} \otimes \mathbf{F})\hat{\mathbf{h}}_{t|t}, \qquad \mathbf{h}_{0|-1} = \mathbf{0}, \tag{38}$$

$$\mathbf{P}_{t+1|t} = (\mathbf{I}_{T_x R_x} \otimes \mathbf{F})(\mathbf{P}_{t|t-1} - \mathbf{K}_t \mathbf{R}_{e,t} \mathbf{K}_t^*)(\mathbf{I}_{T_x R_x} \otimes \mathbf{F}^*) + \mathbf{GR}_u \mathbf{G}^*. \tag{39}$$

Backward run

Starting from $\boldsymbol{\lambda}_{T+1|T} = \mathbf{0}$ *and for* $t = T, T-1, \ldots, 0$, *calculate*

$$
\begin{aligned}
\boldsymbol{\lambda}_{t|T} &= \left(\mathbf{I}_{P+N} - \left(\mathbf{I}_{R_x} \otimes \mathbf{X}_t^*\right)\mathbf{K}_t^*\right)\left(\mathbf{I} \otimes \mathbf{F}^*\right)\boldsymbol{\lambda}_{t+1|T} \\
&\quad + \left(\mathbf{I} \otimes \mathbf{X}_t\right)\mathbf{R}_{e,t}^{-1}\left(\boldsymbol{\mathcal{Y}}_t - \left(\mathbf{I} \otimes \mathbf{X}_t\right)\hat{\mathbf{h}}_{t|t-1}\right),
\end{aligned}
\tag{40}
$$

$$
\hat{\mathbf{h}}_{t|T} = \hat{\mathbf{h}}_{t|t-1} + \mathbf{P}_{t|t-1}\boldsymbol{\lambda}_{t|T}.
\tag{41}
$$

The desired estimate is $\hat{\mathbf{h}}_{t|T}$.

(The Kalman filter has been initialized with zero in (38) as we are dealing with Rayleigh channel. For the case of Ricean channel, we only need to initialize the Kalman filter with nonzero mean corresponding to the direct line-of-sight (LOS) signal present in Ricean channel.) This theorem allows us to obtain the estimate of $\mathbf{h}_0^T$ when the input sequence $\mathbf{X}_0^T$ is not available. For in this case, we maximize the log-likelihood (34) *averaged* over the sequence $\mathbf{X}_0^T$. Thus, the jth iteration of the EM algorithm is now obtained by maximizing the averaged log-likelihood

$$
\overline{\mathcal{L}} = E_{\mathbf{X}_0^T | \boldsymbol{\mathcal{Y}}_0^T, h_0^{T(j-1)}}[\mathcal{L}].
\tag{42}
$$

By inspecting (34), we note that the only term that is modified under expectation is the first summand, and its expectation is given by

$$
\begin{aligned}
&E\left\|\boldsymbol{\mathcal{Y}}_t - \left(\mathbf{I}_{R_x} \otimes \mathbf{X}_t\right)\mathbf{h}_t\right\|_{1/2\sigma_n^2}^2 \\
&= \left\|\boldsymbol{\mathcal{Y}}_t - \left(\mathbf{I}_{R_x} \otimes E[\mathbf{X}_t]\right)\mathbf{h}_t\right\|_{1/2\sigma_n^2}^2 + \left\|\mathbf{h}_t\right\|_{(1/2\sigma_n^2)\mathbf{I}_{R_x} \otimes \mathrm{Cov}[X_t^*]}^2 \\
&= \left\|\begin{bmatrix} \boldsymbol{\mathcal{Y}}_t \\ \mathbf{0}_{T_x R_x(P+1) \times 1} \end{bmatrix} - \begin{bmatrix} \mathbf{I}_{R_x} \otimes E[\mathbf{X}_t] \\ \mathbf{I}_{R_x} \otimes \mathrm{Cov}[\mathbf{X}_t^*]^{1/2} \end{bmatrix}\mathbf{h}_t\right\|_{1/2\sigma_n^2}^2,
\end{aligned}
\tag{43}
$$

where the expectations are taken given the previous estimate $\hat{\mathbf{h}}_0^{(j-1)}$ and the output symbols $\boldsymbol{\mathcal{Y}}_0^T$. We thus have

$$
\begin{aligned}
\overline{\mathcal{L}} &= -\sum_{t=0}^{T}\left\|\begin{bmatrix} \boldsymbol{\mathcal{Y}}_t \\ \mathbf{0}_{T_x R_x(P+1) \times 1} \end{bmatrix} - \begin{bmatrix} \mathbf{I}_{R_x} \otimes E[\mathbf{X}_t] \\ \mathbf{I}_{R_x} \otimes \mathrm{Cov}[\mathbf{X}_t^*]^{1/2} \end{bmatrix}\mathbf{h}_t\right\|_{1/2\sigma_n^2}^2 \\
&\quad - \sum_{t=1}^{T}\left\|\mathbf{h}_t - \mathbf{F}\mathbf{h}_{t-1}\right\|_{(G\mathbf{R}_u G^*)^{-1}}^2 - \left\|\mathbf{h}_0\right\|_{\Pi_0^{-1}}^2.
\end{aligned}
\tag{44}
$$

Note that we can obtain the averaged likelihood (44) from the original likelihood (34) by performing the substitution

$$
\begin{aligned}
\mathbf{I}_{R_x} \otimes \mathbf{X}_t &\longrightarrow \begin{bmatrix} \mathbf{I}_{R_x} \otimes E[\mathbf{X}_t] \\ \mathbf{I}_{R_x} \otimes \mathrm{Cov}[\mathbf{X}_t^*]^{1/2} \end{bmatrix}, \\
\boldsymbol{\mathcal{Y}}_t &\longrightarrow \begin{bmatrix} \boldsymbol{\mathcal{Y}}_t \\ \mathbf{0}_{T_x R_x(P+1) \times 1} \end{bmatrix},
\end{aligned}
\tag{45}
$$

we can thus state the following theorem.

Theorem 2 (channel estimation-unknown input case). *Consider the state-space model (29)-(30) and assume that the receiver does not have access to the transmitted data* $\mathbf{X}_0^T$. *The*

channel estimate at the jth iteration $\mathbf{h}_0^{T(j)}$ of the EM algorithm is obtained by applying the forward-backward Kalman (35)–(41) to the following state-space model

$$
\mathbf{h}_{t+1} = \left(\mathbf{I}_{T_x R_x} \otimes \mathbf{F}\right)\mathbf{h}_t + \left(\mathbf{I}_{T_x R_x} \otimes \mathbf{G}\right)\mathbf{u}_t,
\tag{46}
$$

$$
\begin{bmatrix} \boldsymbol{\mathcal{Y}}_t \\ \mathbf{0}_{T_x R_x(P+1) \times 1} \end{bmatrix} = \begin{bmatrix} \mathbf{I}_{R_x} \otimes E[\mathbf{X}_t] \\ \mathbf{I}_{R_x} \otimes \mathrm{Cov}[\mathbf{X}_t^*]^{1/2} \end{bmatrix}\mathbf{h}_t + \begin{bmatrix} \boldsymbol{\mathcal{N}}_t \\ \underline{\mathbf{n}}_t \end{bmatrix},
\tag{47}
$$

where $\underline{\mathbf{n}}_t$ is virtual noise that is not physically present and that is independent of the physical noise $\boldsymbol{\mathcal{N}}_t$.

The virtual noise results from having a norm of the following form:

$$
\left\|\begin{bmatrix} \boldsymbol{\mathcal{Y}}_t \\ \mathbf{0}_{T_x R_x(P+1) \times 1} \end{bmatrix} - \begin{bmatrix} \mathbf{I}_{R_x} \otimes E[\mathbf{X}_t] \\ \mathbf{I}_{R_x} \otimes \mathrm{Cov}[\mathbf{X}_t^*]^{1/2} \end{bmatrix}\mathbf{h}_t\right\|_{(1/\sigma^2)I}^2.
\tag{48}
$$

Note that the weighting matrix I is now of size $N + P$. To account for this, we assume the presence of virtual noise $\underline{\mathbf{n}}_t$ which is independent of the actual physical noise $\boldsymbol{\mathcal{N}}_t$ in the I/O equation (47).

To fully implement the EM algorithm, we need to initialize the algorithm and calculate the first and second moments of the input, which we do next.

4.3. Initial channel estimation

We obtain the initial channel estimate from the pilot/output equation (18) together with the dynamical channel model (7). Specifically, we do this by applying the FB Kalman to the following state-space model

$$
\mathbf{h}_{t+1} = \left(\mathbf{I}_{T_x R_x} \otimes \mathbf{F}\right)\mathbf{h}_t + \left(\mathbf{I}_{T_x R_x} \otimes \mathbf{G}\right)\mathbf{u}_t,
\tag{49}
$$

$$
\boldsymbol{\mathcal{Y}}_{t_{\mathrm{I}_p}} = \left(\mathbf{I}_{R_x} \otimes \mathbf{X}_{t_{\mathrm{I}_p}}\right)\mathbf{h}_t + \boldsymbol{\mathcal{N}}_{t_{\mathrm{I}_p}},
\tag{50}
$$

that is, by applying the FB Kalman filter (35)–(41) with the following substitution:

$$
\boldsymbol{\mathcal{Y}}_t \longrightarrow \boldsymbol{\mathcal{Y}}_{t_{\mathrm{I}_p}}, \qquad \mathbf{X}_t \longrightarrow \mathbf{X}_{t_{\mathrm{I}_p}}, \qquad \mathbf{I}_{T_x R_x N} \longrightarrow \mathbf{I}_{T_x R_x | I_p|}.
\tag{51}
$$

4.4. Data detection

To detect the data, we use the data detection version of the I/O equation (22). Upon multiplying both sides by $\mathbf{C}^*$ and taking the real part, we obtain

$$
\tilde{\boldsymbol{\mathcal{Y}}} = \|\boldsymbol{\mathcal{H}}\|^2 \begin{bmatrix} \mathrm{Re}\,\boldsymbol{\mathcal{S}} \\ \mathrm{Im}\,\boldsymbol{\mathcal{S}} \end{bmatrix} + \tilde{\boldsymbol{\mathcal{N}}},
\tag{52}
$$

where $\tilde{\boldsymbol{\mathcal{Y}}}$ and $\tilde{\boldsymbol{\mathcal{N}}}$ are $2N_u \times 1$ vectors defined by $\tilde{\boldsymbol{\mathcal{Y}}} = \mathrm{Re}\mathbf{C}^*\boldsymbol{\mathcal{Y}}$ and $\tilde{\boldsymbol{\mathcal{N}}} = \mathrm{Re}\mathbf{C}^*\boldsymbol{\mathcal{N}}$. Since $\mathbf{C}$ is orthogonal, the noise $\tilde{\boldsymbol{\mathcal{N}}}$ remains white, and the input can be detected on an element-by-element basis. (Equation (13) holds for every STBC but only the orthogonal case is considered in this work.) We will now demonstrate how to detect the elements of $\mathrm{Re}\,\boldsymbol{\mathcal{S}}$ (the imaginary part can be treated similarly). So let $\mathcal{R} = \{r_1, \ldots, r_{|\mathcal{R}|}\}$ denote the alphabet set from which the elements of $\mathrm{Re}\,\boldsymbol{\mathcal{S}}$ take their values. We can evaluate the

conditional pdf $f(\mathrm{Re}\,\boldsymbol{\mathcal{S}}(n_u)|\widetilde{\boldsymbol{\mathcal{Y}}}(n_u),\boldsymbol{\mathcal{H}})$ by applying Bayes rule on it which yields

$$
\begin{aligned}
f(r_i \mid \widetilde{\boldsymbol{\mathcal{Y}}}(n_u),\boldsymbol{\mathcal{H}}) &= \frac{f(r_i,\widetilde{\boldsymbol{\mathcal{Y}}}(n_u) \mid \boldsymbol{\mathcal{H}})}{f(\widetilde{\boldsymbol{\mathcal{Y}}}(n_u) \mid \boldsymbol{\mathcal{H}})} \\
&= \frac{f(r_i,\widetilde{\boldsymbol{\mathcal{Y}}}(n_u) \mid \boldsymbol{\mathcal{H}})}{\sum_{i=1}^{|\mathcal{R}|} f(\widetilde{\boldsymbol{\mathcal{Y}}}(n_u),r_i \mid \boldsymbol{\mathcal{H}})} \\
&= \frac{f(\widetilde{\boldsymbol{\mathcal{Y}}}(n_u) \mid r_i,\boldsymbol{\mathcal{H}})f(r_i \mid \boldsymbol{\mathcal{H}})}{\sum_{i=1}^{|\mathcal{R}|} f(\widetilde{\boldsymbol{\mathcal{Y}}}(n_u) \mid r_i,\boldsymbol{\mathcal{H}})f(r_i \mid \boldsymbol{\mathcal{H}})},
\end{aligned}
\tag{53}
$$

$$
f(r_i \mid \widetilde{\boldsymbol{\mathcal{Y}}}(n_u),\boldsymbol{\mathcal{H}}) = \frac{e^{-(|\widetilde{\boldsymbol{\mathcal{Y}}}(n_u)-\|\boldsymbol{\mathcal{H}}\|^2 r_i|^2)/2\sigma_n^2}}{\sum_{i=1}^{|\mathcal{R}|} e^{-(|\widetilde{\boldsymbol{\mathcal{Y}}}(n_u)-\|\boldsymbol{\mathcal{H}}\|^2 r_i|^2)/2\sigma_n^2}}.
\tag{54}
$$

We can use this pdf to calculate conditional expectation of $\mathrm{Re}\,\boldsymbol{\mathcal{S}}(n_u)$ and its second moment given the output $\widetilde{\boldsymbol{\mathcal{Y}}}(n_u)$:

$$
E[\mathrm{Re}\,\boldsymbol{\mathcal{S}}(n_u) \mid \widetilde{\boldsymbol{\mathcal{Y}}}(n_u),\boldsymbol{\mathcal{H}}] = \frac{\sum_{i=1}^{|\mathcal{R}|} r_i e^{-(|\widetilde{\boldsymbol{\mathcal{Y}}}(n_u)-\|\boldsymbol{\mathcal{H}}\|^2 r_i|^2)/2\sigma_n^2}}{\sum_{i=1}^{|\mathcal{R}|} e^{-(|\widetilde{\boldsymbol{\mathcal{Y}}}(n_u)-\|\boldsymbol{\mathcal{H}}\|^2 r_i|^2)/2\sigma_n^2}},
$$

$$
E\big[|\mathrm{Re}\,\boldsymbol{\mathcal{S}}(n_u)|^2 \mid \widetilde{\boldsymbol{\mathcal{Y}}}(n_u),\boldsymbol{\mathcal{H}}\big] = \frac{\sum_{i=1}^{|\mathcal{R}|} r_i^2 e^{-(|\widetilde{\boldsymbol{\mathcal{Y}}}(n_u)-\|\boldsymbol{\mathcal{H}}\|^2 r_i|^2)/2\sigma_n^2}}{\sum_{i=1}^{|\mathcal{R}|} e^{-(|\widetilde{\boldsymbol{\mathcal{Y}}}(n_u)-\|\boldsymbol{\mathcal{H}}\|^2 r_i|^2)/2\sigma_n^2}}.
\tag{55}
$$

We can similarly calculate the two moments of the imaginary part. Now (55), just like (19)–(24), apply at a certain frequency tone n. So collecting (55) for all tones $(n = 1,\ldots,N)$ produces the two moments of the uncoded OFDM symbols. Specifically, we can calculate

$$
\begin{array}{ll}
E[\mathrm{Re}\,\boldsymbol{\mathcal{S}}(n_u)], & E[\mathrm{Im}\,\boldsymbol{\mathcal{S}}(n_u)], \\
E[\mathrm{diag}(\mathrm{Re}\,\boldsymbol{\mathcal{S}}(n_u))^2], & E[\mathrm{diag}(\mathrm{Im}\,\boldsymbol{\mathcal{S}}(n_u))^2].
\end{array}
\tag{56}
$$

We show in Appendix B that these moments are enough to characterize the first and second moments $E[\mathbf{X}]$ and $E[\mathbf{X}^*\mathbf{X}]$, which are needed for channel estimation.

4.5. Summary of the EM-based receiver

We now have all the elements for the iterative receiver for channel and data recovery, and for ease of reference, we summarize the receiver algorithm in the following. Given a sequence of input and output symbols $\mathbf{X}_0^T$ and $\boldsymbol{\mathcal{Y}}_0^T$ perform the following operations.

(1) Calculate the initial channel estimate $\mathbf{h}_0^T(0)$ by applying the FB Kalman filter to the state-space model (49)-(50), that is, by applying (35)–(41) with the following substitutions:

$$
\boldsymbol{\mathcal{Y}}_t \longrightarrow \boldsymbol{\mathcal{Y}}_{t_{I_\mathrm{p}}}, \qquad \mathbf{X}_t \longrightarrow \mathbf{X}_{t_{I_\mathrm{p}}}, \qquad \mathbf{I}_{T_x R_x N} \longrightarrow \mathbf{I}_{T_x R_x |I_\mathrm{p}|}.
\tag{57}
$$

(2) Iterate between the expectation and maximization steps for $j = 1,\ldots,N_\mathrm{iter}$:

(a) expectation:

(i) use (55) to compute the first two moments of the uncoded OFDM symbols $\boldsymbol{\mathcal{S}}(1),\ldots,\boldsymbol{\mathcal{S}}(n_u)$, given the output $\boldsymbol{\mathcal{Y}}_0^T$ and the most recent estimate of the channel, $\mathbf{h}_0^T(j-1)$;

(ii) use these moments to calculate the moments of $\mathbf{X}$ through the relationships (13) and (55).

(b) maximization:

obtain the channel estimate $\mathbf{h}_0^T(j)$ by employing the FB Kalman to the state-space model (46)-(47), that is, by applying (35)–(41) with the following substitutions:

$$
\begin{aligned}
\mathbf{I}_{R_x} \otimes \mathbf{X}_t &\longrightarrow \begin{bmatrix} \mathbf{I}_{R_x} \otimes E[\mathbf{X}_t] \\ \mathbf{I}_{R_x} \otimes \mathrm{Cov}[\mathbf{X}_t^*]^{1/2} \end{bmatrix}, \\
\boldsymbol{\mathcal{Y}}_t &\longrightarrow \begin{bmatrix} \boldsymbol{\mathcal{Y}}_t \\ \mathbf{0}_{T_x R_x (P+1) \times 1} \end{bmatrix}, \\
\mathbf{I}_{T_x R_x N} &\longrightarrow \mathbf{I}_{T_x R_x (N+P+1)}.
\end{aligned}
\tag{58}
$$

The algorithm can be stopped when the maximum number of iterations N_iter is reached or when the difference between two consecutive estimates $\|\mathbf{h}_0^{T(j)} - \mathbf{h}_0^{T(j-1)}\|^2$ is below a certain threshold.

4.6. Modification: Kalman- (forward-only) based estimation

One disadvantage of the FB Kalman (summarized in Section 4.5 above) is the storage and latency involved. The algorithm needs to wait for all $T + 1$ ST symbols before it can execute the backward run and hence obtain the channel estimate. One way around this is to reduce the window size T. Alternatively, we can run the filter in the forward direction only (i.e., run (35)–(39)) for both the initial estimation and the EM iteration. The algorithm then collapses to the Kalman-based filter proposed in [34] where the data and channel are recovered within one ST symbol.

5. SIMULATION RESULTS

In the following simulations, we test the performance of the forward and forward-backward Kalman filters.

5.1. The forward-only Kalman

The transmitter and receiver illustrated in Figures 1 and 2 were implemented. The outer encoder is a rate 3/4 convolutional encoder and the coded bits are mapped to 16-QAM symbols using Gray coding. We use the OSTBC commonly known as the Alamouti code with number of time slots $N_s = 2$ and number of transmitters $T_x = 2$ [35].

Our MIMO channel model is simulated using the state-space model (7) with parameters, $\alpha = 0.985$, $\beta = 0.2$, and $P = 7$. The number of receive antennas is set to $R_x = 2$.

Three thousand packets were simulated per SNR-value. Each packet is comprised of 12 OFDM symbols transmitted over six ST blocks. Each OFDM symbol consists of 64 frequency tones and a cyclic prefix of length 16. The length of cyclic prefix is always kept greater than or equal to the channel length $P + 1$ to avoid any ISI. We employ 16 pilots in the OFDM symbols making up the first ST block, while the number of pilots we use in subsequent symbols vary between two, six, and ten.

In the following, we discuss the effect of various parameters on the BER performance of the receiver design.

5.1.1. Bench marking

We compare our algorithm with an EM-based iterative MMSE receiver such as the one proposed in [17, 21]. In contrast to our work, the authors in [17, 21] take a data-centric approach, treating the transmitted signal as the desired parameter and the channel as the unobserved data. This algorithm further confines its pilots to the first ST block. The pilots are used to produce an initial channel estimate for the first ST block. This estimate is in turn used to predict the initial channel estimate for the subsequent ST blocks by employing a time correlation filter [17]. These initial estimates are used to kick-start the EM algorithm.

In this algorithm, the E-step is calculated by a conditional expectation of the channel given the received symbol and the current estimate of the transmitted data (i.e., through MMSE estimation). The maximization step is simply the hard decision, that is, the ML estimate of the transmitted data.

In Figure 3, we compare both schemes with 16 pilots in the initial ST block and zero pilots in the subsequent blocks. EM_A refers to the iterative MMSE scheme while EM_B refers to the Kalman filter-based scheme proposed in this paper. We also implement both schemes with a total of 26 pilots as shown in Figure 3. The EM_A confines the pilots to the first ST block while in EM_B, we place 16 pilots in the first ST block and 2 pilots each in subsequent blocks. This ensures that both schemes incur the same pilot overhead.

Our algorithm (EM_B) outperforms EM_A of [17] in both pilot scenarios. One reason for this performance improvement is that our algorithm incorporates the time correlation information and the most recent channel estimate in *every* iteration of the EM algorithm, while that of [17] does not.
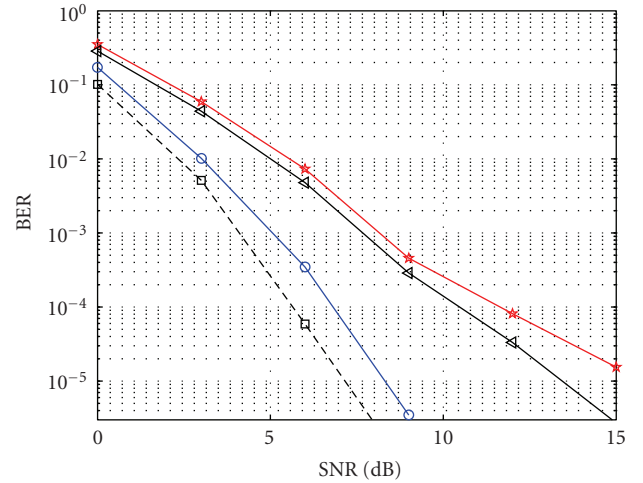
5.1.2. Effect of number of iterations

In this section, we test the sensitivity of our algorithm to the number of EM iterations used. Here, we employ six pilots per OFDM symbol (in addition to the 16 pilots per symbol employed in the first ST block). From Figure 4, we see that the first iteration yields substantial improvement over the pilot-based estimation. The enhanced performance with increased number of EM iterations is also evident from Figure 4. This improved performance comes at the cost of increased computational complexity.

FIGURE 3: Comparison of EM-MMSE(EM_A) and EM-FB-Kalman (EM_B) algorithms.
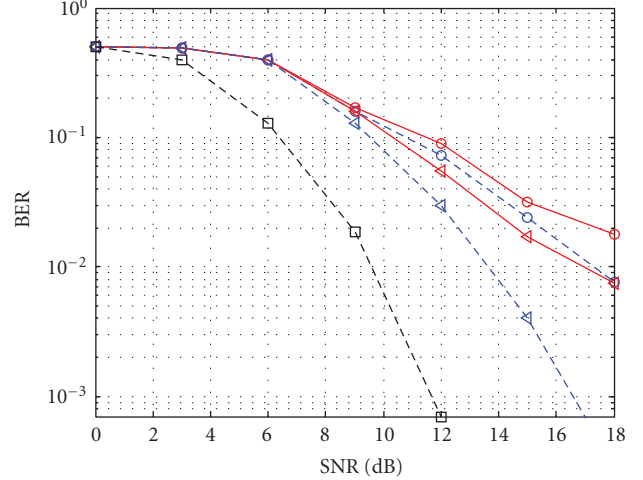
Legend:
- EM_A, pilots = [16 0 0 0 0 0 0]
- EM_B, pilots = [16 0 0 0 0 0 0]
- EM_A, pilots = [26 0 0 0 0 0 0]
- EM_B, pilots = [16 2 2 2 2 2 2]
- Perf. ch.

FIGURE 4: BER performance with different number of EM iterations.

Legend:
- Pilots only
- Iter = 1
- Iter = 4
- Perf. ch.

5.1.3. Effect of incorporating frequency and time correlation in the channel estimation

The impact of using both frequency and time correlations in channel estimation is shown in Figure 5 for the six-pilot scenario. In this figure, $I_e = 1$ (where I_e stands for "information used in estimation") refers to channel estimation using either frequency or time correlation information only while $I_e = 2$ implies the use of both frequency and time correlation in channel estimation. We observe an error floor when either the frequency or time correlation information is
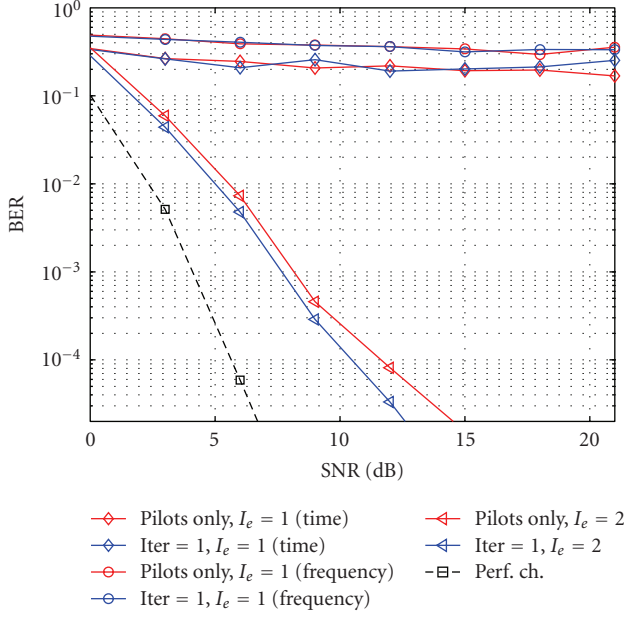
FIGURE 5: Effect of a priori correlation knowledge on the performance of the receiver.

FIGURE 6: BER performance with varying time correlation with six pilots.

used in channel estimation. (By using frequency correlation only, we mean a receiver that estimates the channel using least squares, i.e., by performing the minimization in (28). This could equivalently be performed by implementing the FB-Kalman (35)–(41) with the matrix $\mathbf{F}$ set to zero. Similarly, the time correlation only case can be performed by implementing the FB-Kalman (35)–(41) with the matrix $\mathbf{G}$ set to $\sqrt{1 - \alpha^2(p)}\mathbf{I}$. It should be clear that it is not possible to ignore the frequency correlation completely but by using this setting, its effect is only decreased as the channel taps do not follow the exponential channel decay profile and become identically distributed.) This error floor remains regardless of the number of iterations. However, when we incorporate both frequency and time correlation information, we observe a significant improvement in BER. We also note that a single EM iteration provides substantial improvement when compared to the pilot-based estimation case. We conclude that including both time and frequency correlations in the channel estimation process (especially for channels with high time correlation) increases the amount of information that can be harnessed by iterating.

5.1.4. Effect of time variation

In this section, we test the performance of our receiver against different degrees of time variation. This is parameterized by α ($0 \le \alpha \le 1$) with lower values of α indicating a more time-variant channel. (According to IEEE 802.16 standards, the typical range for α is 0.677 to 0.9398 for a vehicle speed decreasing from 120 km/h to 50 km/h, resp.) In Figure 6, we show the BER curves for a system that employs six pilots per OFDM symbol. We observe an error floor as the channel variation increases. So, we are unable to capture the time
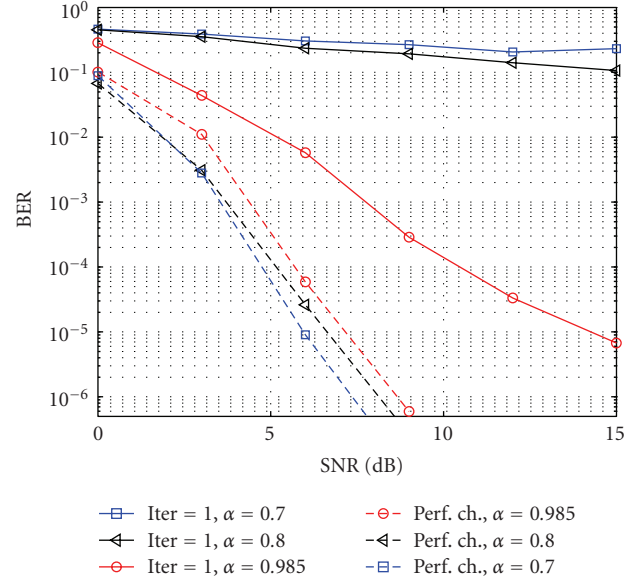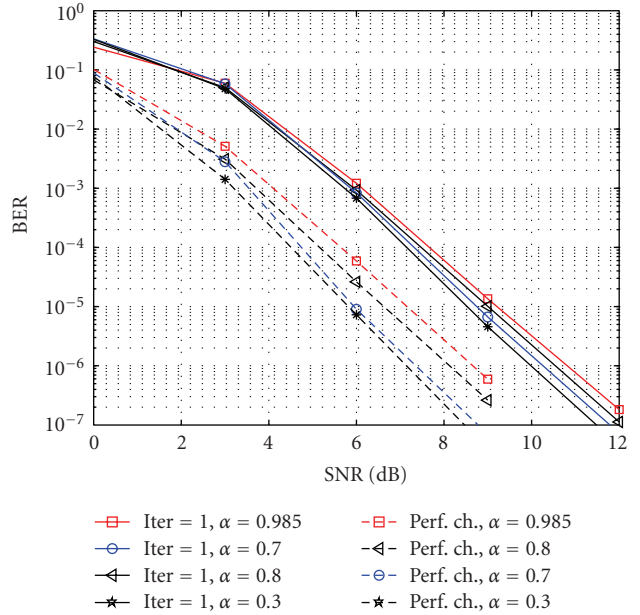

FIGURE 7: BER performance with varying time correlation with ten pilots.

diversity. More pilots are thus needed to capture diversity and improve performance.

For comparison, in Figure 7, we show the BER curves for a system with ten pilots per OFDM symbol for $\alpha = 0.3, 0.7, 0.8$ and 0.985. From this figure, we observe that as α decreases (indicating more channel variation), the BER improves. This comes from increased time diversity in the channel. Therefore, with enough number of pilots, we are able to track the channel and capture time diversity.
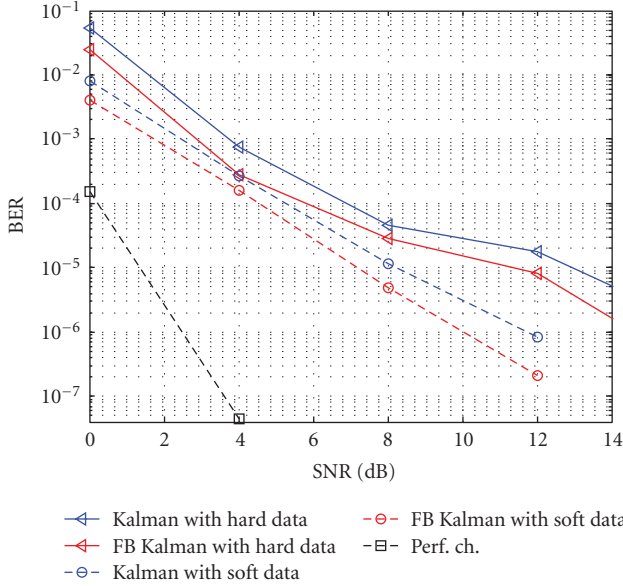
FIGURE 8: BER performance of Kalman and FB-Kalman using hard and soft estimate of data.

5.2. The FB Kalman

To test the FB Kalman filter, we use an input similar to the one employed in the forward-only Kalman case. The outer encoder in this case is a rate 1/2 convolutional encoder. The number of transmitters is two as Alamouti code is used in this case also and the number of receivers is also fixed at two. We use two MIMO channel models in this case. One is spatially white while the other one is spatially correlated with transmit and receive correlation matrices

$$\mathbf{T}(p) = \begin{bmatrix} 1 & \zeta \\ \zeta & 1 \end{bmatrix}, \qquad \mathbf{R}(p) = I, \qquad (59)$$

where $\zeta = 0.2$. All other parameters are the same in both channel models, that is, $\alpha = 0.8$, $\beta = 0.2$, and $P = 16$.

Packets are transmitted at each SNR-value until a minimum number of errors (five in this case) occur. Similar to the forward-only Kalman case, each packet consists of six ST blocks. The first ST block contains 16 pilots while the number of pilots in subsequent blocks remains fixed at 12.

Figure 8 compares the Kalman and the FB-Kalman over spatially white channel. The results are shown for two scenarios. In one, hard estimate of data (the estimated data) is used while in the other soft estimate (expected value of the data) is used. The figure clearly illustrates that the FB-Kalman is better than the Kalman for both scenarios. It can also be observed from this figure that the FB-Kalman using soft estimate of data outperforms the one using hard estimate.

The performance of Kalman and the FB-Kalman is compared in Figure 9 over the two channel models, that is, spatially correlated and spatially white channel model. In both cases, soft estimate of data is used. In the perfect channel scenario, the increased diversity in uncorrelated (white) case gives a better BER compared to the correlated case. However, in the estimated channel case, diversity is
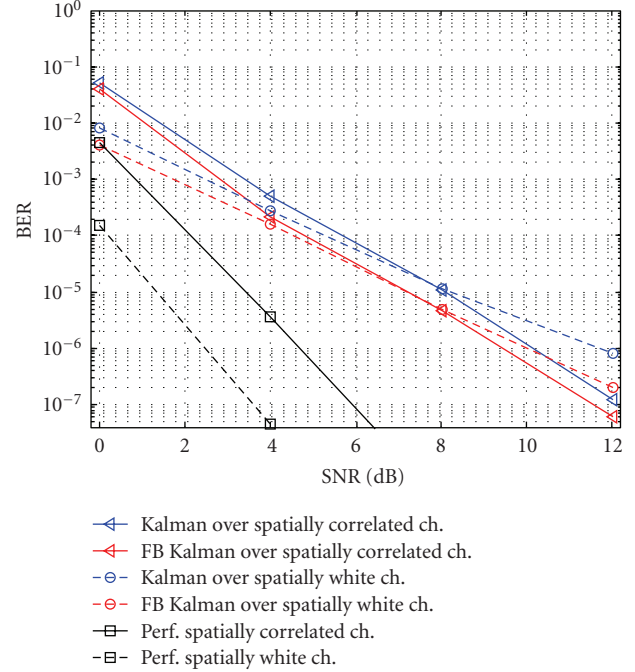

FIGURE 9: BER performance of Kalman and FB-Kalman using soft data over spatially white and correlated channel models.

a two-edged sword. On the one hand, increased diversity should improve performance if we manage to have a good estimate of the channel. On the other hand, increased diversity also increases the channel's degrees of freedom giving an inferior estimate to the uncorrelated case for the same number of pilots used. This explains why in the estimated case, the correlated channel performs better than the uncorrelated channel for the channel estimate quality in the former is better than the channel quality in the latter.

6. CONCLUSION

In this paper, we have proposed a receiver for MIMO-OFDM transmission over time-variant channels. While the paper assumed the channel to be constant within any ST block, the channel was allowed to vary from one block to the next. This makes the receiver suitable for operation in high-speed environments.

The receiver employs the EM algorithm to achieve channel and data recovery. Specifically, the data recovery (or the expectation step) is as simple as decoding a space-time block code. Channel recovery (or the maximization step) is performed using a forward-backward Kalman filter. We also suggested a relaxed (forward-only) version of the algorithm that is able to perform recovery with no latency and hence avoid the delay and storage shortcomings of the FB-Kalman.

When compared with other MIMO receivers, our receiver makes the most use of the underlying structure. Specifically, the algorithm makes use of the finite alphabet constraints (55), the data in its soft form (46)-(47), pilots (49)-(50), finite-delay spread (in that channel estimation is done in the time domain), frequency and time correlation (7), spatial

correlation in (A.16), and space-time coding. It is also straightforward to incorporate the effect of an outer code, sparsity, and the cyclic prefix (see [27, 36]). Our simulations show the favorable behavior of the two Kalman filters as compared to other receivers.

APPENDICES

A. CHANNEL MODEL IN THE PRESENCE OF SPATIAL CORRELATION

In what follows, we derive the dynamical model for the channel impulse response in the transmit correlation case, and then generalize our results of Section 2.2 to deal with the general (transmit and receive) correlation case. In the transmit correlation case, H(p), the MIMO impulse response at tap p, is given by

$$\mathbf{H}(p) = \mathbf{W}(p)\mathbf{T}^{1/2}(p), \qquad (A.1)$$

where $\mathbf{T}^{1/2}(p)$ is the transmit correlation matrix (of size T_x) at tap p and where $\mathbf{W}(p)$ consists of iid elements. The matrix $\mathbf{W}(p)$ remains constant over a single ST block and varies from one ST block to the next according to

$$\mathbf{W}_{t+1}(p) = \alpha(p)\mathbf{W}_t(p) + \sqrt{(1-\alpha^2(p))e^{-\beta p}}\mathbf{U}_t(p), \quad (A.2)$$

where $\alpha(p), \beta$, and $\mathbf{U}_t(p)$ are as defined in Section 2.2. (We suppress the time dependence at times for notational convenience.)

Just as we did in Section 2.2, we would like to construct a recursion for the tap $h_{r_x}^{t_x}(p)$ and subsequently scale it up for the SISO and MIMO cases. Now since $h_{r_x}^{t_x}(p)$ is the (r_x, t_x) element of $\mathbf{H}(p)$, we deduce from (A.1) that it is the inner product of the r_x row of $\mathbf{W}(p)$ and the t_x column of $\mathbf{T}^{1/2}$, that is,

$$h_{r_x}^{t_x}(p) = \mathbf{w}_{r_x}(p)\mathbf{t}^{t_x}(p). \qquad (A.3)$$

Moreover, from (A.2), we have the following recursion for $\mathbf{w}_{r_x}(p)$:

$$\mathbf{w}_{r_x,t+1}(p) = \alpha(p)\mathbf{w}_{r_x,t}(p) + \sqrt{(1-\alpha^2(p))e^{-\beta p}}\mathbf{u}_{r_x,t}(p). \qquad (A.4)$$

Postmultiplying both sides by $\mathbf{t}^{t_x}(p)$ yields

$$\mathbf{w}_{r_x,t+1}(p)\mathbf{t}^{t_x}(p) = \alpha(p)\mathbf{w}_{r_x,t}(p)\mathbf{t}^{t_x}(p) \\ + \sqrt{(1-\alpha^2(p))e^{-\beta p}}\mathbf{u}_{r_x,t}(p)\mathbf{t}^{t_x}(p). \qquad (A.5)$$

This means that $h_{r_x}^{t_x}(p)$ satisfies the dynamical equation

$$h_{r_x,t+1}^{t_x}(p) = \alpha(p)h_{r_x,t}^{t_x}(p) + \sqrt{(1-\alpha^2(p))e^{-\beta p}}ut_{r_x,t}^{t_x}(p), \qquad (A.6)$$

where $ut_{r_x}^{t_x}$ is defined by

$$ut_{r_x}^{t_x}(p) = \mathbf{u}_{r_x}(p)\mathbf{t}^{t_x}(p). \qquad (A.7)$$

Concatenating (A.6) for $p = 1, 2, \ldots, P$ yields a dynamic equation for the impulse response

$$\mathbf{h}_{r_x}^{t_x} = \begin{bmatrix} h_{r_x}^{t_x}(0) \\ \vdots \\ h_{r_x}^{t_x}(P) \end{bmatrix} = \begin{bmatrix} \mathbf{w}_{r_x}(0)\mathbf{t}^{t_x}(0) \\ \vdots \\ \mathbf{w}_{r_x}(P)\mathbf{t}^{t_x}(P) \end{bmatrix}, \qquad (A.8)$$

which is the same as the dynamic equation (see (5)) for the spatially uncorrelated case

$$\mathbf{h}_{r_x,t+1}^{t_x} = \mathbf{F}\mathbf{h}_{r_x,t}^{t_x} + \mathbf{G}ut_{r_x,t}^{t_x}. \qquad (A.9)$$

The only difference from the uncorrelated case is that $\mathbf{ut}_{r_x}^{t_x}$ is no more white. Rather, we have

$$\begin{aligned} E\big[&\mathbf{ut}_{r_x}^{t_x}\mathbf{ut}_{r_x}^{t_x*}\big] \\ &\triangleq E\begin{bmatrix} \mathbf{u}_{r_x}(0)\mathbf{t}^{t_x}(0) \\ \mathbf{u}_{r_x}(1)\mathbf{t}^{t_x}(1) \\ \vdots \\ \mathbf{u}_{r_x}(P)\mathbf{t}^{t_x}(P) \end{bmatrix} \\ &\quad \times \begin{bmatrix} \mathbf{t}^{t_x*}(0)\mathbf{u}_{r_x}^*(0) & \mathbf{t}^{t_x*}(1)\mathbf{u}_{r_x}^*(1) & \cdots & \mathbf{t}^{t_x*}(P)\mathbf{u}_{r_x}^*(P) \end{bmatrix} \\ &= \begin{bmatrix} \mathbf{tt}_{t_x}^{t_x}(0) & & & \\ & \mathbf{tt}_{t_x}^{t_x}(1) & & \\ & & \ddots & \\ & & & \mathbf{tt}_{t_x}^{t_x}(P) \end{bmatrix} \triangleq \mathrm{diag}(\mathbf{tt}_{t_x}^{t_x}), \end{aligned}$$
$$(A.10)$$

where

$$\mathbf{tt}_{r_x}^{t_x} = \begin{bmatrix} \mathbf{t}^{r_x*}(0)\mathbf{t}^{t_x}(0) \\ \mathbf{t}^{r_x*}(1)\mathbf{t}^{t_x}(1) \\ \vdots \\ \mathbf{t}^{r_x*}(P)\mathbf{t}^{t_x}(P) \end{bmatrix} = \begin{bmatrix} \mathbf{t}_{r_x}(0)\mathbf{t}^{t_x}(0) \\ \mathbf{t}_{r_x}(1)\mathbf{t}^{t_x}(1) \\ \vdots \\ \mathbf{t}_{r_x}(P)\mathbf{t}^{t_x}(P) \end{bmatrix}, \qquad (A.11)$$

and where the second line follows from the fact that $\mathbf{t}^{r_x*}(p) = \mathbf{t}_{t_x}(p)$ since $\mathbf{T}^{1/2}(p)$ is conjugate symmetric. In general, we can show that

$$E\big[\mathbf{ut}_{r_x}\mathbf{ut}_{r_x}^*\big] = \begin{bmatrix} \mathrm{diag}(\mathbf{tt}_1^1) & \mathrm{diag}(\mathbf{tt}_1^2) & \cdots & \mathrm{diag}(\mathbf{tt}_1^{T_x}) \\ \mathrm{diag}(\mathbf{tt}_2^1) & \mathrm{diag}(\mathbf{tt}_2^2) & \cdots & \mathrm{diag}(\mathbf{tt}_2^{T_x}) \\ \vdots & \vdots & \cdots & \vdots \\ \mathrm{diag}(\mathbf{tt}_{T_x}^1) & \mathrm{diag}(\mathbf{tt}_{T_x}^2) & \cdots & \mathrm{diag}(\mathbf{tt}_{T_x}^{T_x}) \end{bmatrix}, \qquad (A.12)$$

for $r_x = r_x'$ and is zero otherwise. Alternatively, we can write this as

$$E\big[\mathbf{ut}_{r_x}\mathbf{ut}_{r_x'}^*\big] = \begin{cases} \sum_{p=0}^{P}\mathbf{T}(p) \otimes (\underline{\mathbf{I}}^p \mathbf{B}\overline{\mathbf{I}}^p) & \text{for } r_x = r_x', \\ \mathbf{O} & \text{otherwise,} \end{cases} \qquad (A.13)$$

where

$$\mathbf{B} = \begin{bmatrix} 1 & 0 & \cdots & 0 \\ 0 & 0 & \cdots & 0 \\ \vdots & \vdots & \cdots & \vdots \\ 0 & 0 & \cdots & 0 \end{bmatrix},$$

$$\underline{\mathbf{I}} = \begin{bmatrix} 0 & & & & \\ 1 & 0 & & & \\ & 1 & \ddots & & \\ & & \ddots & 0 & \\ & & & 1 & 0 \end{bmatrix},$$

$$\bar{\mathbf{I}} = \begin{bmatrix} 0 & 1 & & & \\ & 0 & \ddots & & \\ & & \ddots & 1 & \\ & & & 0 & 1 \\ & & & & 0 \end{bmatrix}. \tag{A.14}$$

Collecting (A.9) for all transmit and receive antennas yields

$$\mathbf{h}_{t+1} = (\mathbf{I}_{T_x R_x} \otimes \mathbf{F})\mathbf{h}_t + (\mathbf{I}_{T_x R_x} \otimes \mathbf{G})\mathbf{ut}_t, \tag{A.15}$$

where

$$\begin{aligned} E[\mathbf{uu}^*] &= \mathbf{I}_{R_x} \otimes E[\mathbf{ut}_{r_x} \mathbf{ut}_{r_x}^*] \\ &= \sum_{p=0}^{P} \mathbf{I}_{R_x} \otimes \mathbf{T}(p) \otimes (\underline{\mathbf{I}}^p \mathbf{B} \bar{\mathbf{I}}^p). \end{aligned} \tag{A.16}$$

When the channel exhibits both transmit and receive correlations, the IR**h** continues to satisfy the dynamical equation (A.15) except that the correlation of the innovation **u** is now given by

$$E[\mathbf{uu}^*] = \sum_{p=0}^{P} \mathbf{R}(p) \otimes \mathbf{T}(p) \otimes (\underline{\mathbf{I}}^p \mathbf{B} \bar{\mathbf{I}}^p). \tag{A.17}$$

B. CALCULATING THE MOMENTS OF $\mathbf{X}$

In this appendix, we demonstrate that the four moments (56) of the uncoded OFDM symbol $\pmb{\delta}(n_u)$ are enough to calculate the first two moments of $\mathbf{X}$, $E[\mathbf{X}]$, and $E[\mathbf{X}^*\mathbf{X}]$. Since $\mathbf{X}$ depends linearly on $\mathrm{Re}\,\pmb{\delta}(n_u)$ and $\mathrm{Im}\,\pmb{\delta}(n_u)$ (see (13) and (16)), it is straight forward to calculate the mean of $\mathbf{X}$ starting from the means of $\mathrm{Re}\,\pmb{\delta}(n_u)$ and $\mathrm{Im}\,\pmb{\delta}(n_u)$. Now from (16), we note that evaluating $E[\mathbf{X}^*\mathbf{X}]$ boils down to evaluating the cross correlation $E[\mathrm{diag}(\pmb{\mathcal{X}}_i^*(n_c))\mathrm{diag}(\pmb{\mathcal{X}}_j(n_c'))]$, recall also that

$$\pmb{\mathcal{X}}_{t_x}(n_c) = \sum_{n_u=1}^{N_u} a_{t_x,n_c}(n_u)\mathrm{Re}\,\pmb{\delta}(n_u) + jb_{t_x,n_c}(n_u)\mathrm{Im}\,\pmb{\delta}(n_u). \tag{B.1}$$

This means that calculating the cross expectation boils down to calculating the cross correlation of $\mathrm{Re}\,\pmb{\delta}(n_u), \mathrm{Im}\,\pmb{\delta}(n_u)$, $\mathrm{Re}\,\pmb{\delta}(n_u')$, and $\mathrm{Im}\,\pmb{\delta}(n_u')$ for $n_u, n_u' = 1, \ldots, N_u$. It is easy

to see that these variables are independent for $n_u \neq n_u'$. Moreover, since the noise in (52) is white, one can also see that $\mathrm{Re}\,\pmb{\delta}(n_u)$ and $\mathrm{Im}\,\pmb{\delta}(n_u)$ are independent. As a result, we can completely characterize the cross correlation $E[\mathrm{diag}(\pmb{\mathcal{X}}_i^*(n_c))\mathrm{diag}(\pmb{\mathcal{X}}_j(n_c'))]$ and hence the expectations $E[\mathbf{X}]$ and $E[\mathbf{X}^*\mathbf{X}]$ starting from the first and second moments of (56).

REFERENCES

[1] A. Paulraj, R. Nabar, and D. Gore, *Introduction to Space Time Wireless Communications*, Cambridge University Press, Cambridge, UK, 2003.

[2] Y. Li, N. Seshadri, and S. Ariyavisitakul, "Channel estimation for OFDM systems with transmitter diversity in mobile wireless channels," *IEEE Journal on Selected Areas in Communications*, vol. 17, no. 3, pp. 461–471, 1999.

[3] R. Negi and J. Cioffi, "Pilot tone selection for channel estimation in a mobile OFDM system," *IEEE Transactions on Consumer Electronics*, vol. 44, no. 3, pp. 1122–1128, 1998.

[4] F. Tufvesson and T. Maseng, "Pilot assisted channel estimation for OFDM in mobile cellular systems," in *Proceedings of the 47th IEEE Vehicular Technology Conference (VTC '97)*, vol. 3, pp. 1639–1643, Phoenix, Ariz, USA, May 1997.

[5] S. Ohno and G. B. Giannakis, "Optimal training and redundant precoding for block transmissions with application to wireless OFDM," *IEEE Transactions on Communications*, vol. 50, no. 12, pp. 2113–2123, 2002.

[6] Y. Li, "Pilot-symbol-aided channel estimation for OFDM in wireless systems," in *Proceedings of the 49th IEEE Annual Vehicular Technology Conference (VTC '99)*, vol. 2, pp. 1131–1135, Houston, Tex, USA, May 1999.

[7] I. Barhumi, G. Leus, and M. Moonen, "Optimal training design for MIMO OFDM systems in mobile wireless channels," *IEEE Transactions on Signal Processing*, vol. 51, no. 6, pp. 1615–1624, 2003.

[8] R. W. Heath Jr. and G. B. Giannakis, "Exploiting input cyclostationarity for blind channel identification in OFDM systems," *IEEE Transactions on Signal Processing*, vol. 47, no. 3, pp. 848–856, 1999.

[9] B. Muquet, M. de Courville, P. Duhamel, and V. Buzenac, "A subspace based blind and semi-blind channel identification method for OFDM systems," in *Proceedings of the 2nd IEEE Workshop on Signal Processing Advances in Wireless Communications (SPAWC '99)*, pp. 170–173, Annapolis, Md, USA, May 1999.

[10] H. Bölcskei, R. W. Heath Jr., and A. J. Paulraj, "Blind channel identification and equalization in OFDM-based multiantenna systems," *IEEE Transactions on Signal Processing*, vol. 50, no. 1, pp. 96–109, 2002.

[11] Z. Liu, G. B. Giannakis, A. Scaglione, and S. Barbarossa, "Decoding and equalization of unknown multipath channels

based on block precoding and transmit-antenna diversity," in *Proceedings of the 33rd Asilomar Conference on Signals, Systems and Computers*, vol. 2, pp. 1557–1561, Pacific Grove, Calif, USA, October 1999.

[12] S. Zhou, B. Muquet, and G. B. Giannakis, "Subspace-based (semi-) blind channel estimation for block precoded space-time OFDM," *IEEE Transactions on Signal Processing*, vol. 50, no. 5, pp. 1215–1228, 2002.

[13] S. Zhou and G. B. Giannakis, "Finite-alphabet based channel estimation for OFDM and related multicarrier systems," *IEEE Transactions on Communications*, vol. 49, no. 8, pp. 1402–1414, 2001.

[14] O. Edfors, M. Sandell, J.-J. van de Beek, S. K. Wilson, and P. O. Borjesson, "OFDM channel estimation by singular value decomposition," *IEEE Transactions on Communications*, vol. 46, no. 7, pp. 931–939, 1998.

[15] B. Yang, K. B. Letaief, R. S. Cheng, and C. Zhigang, "Channel estimation for OFDM transmission in multipath fading channels based on parametric channel modeling," *IEEE Transactions on Communications*, vol. 49, no. 3, pp. 467–479, 2001.

[16] T. Y. Al-Naffouri, A. Bahai, and A. Paulraj, "Semi-blind channel identification and equalization in OFDM: an expectation-maximization approach," in *Proceedings of the 56th Vehicular Technology Conference (VTC '02)*, vol. 1, pp. 13–17, Vancouver, Canada, September 2002.

[17] B. Lu, X. Wang, and Y. Li, "Iterative receivers for space-time block-coded OFDM systems in dispersive fading channels," *IEEE Transactions on Wireless Communications*, vol. 1, no. 2, pp. 213–225, 2002.

[18] Y. Li, C. N. Georghiades, and G. Huang, "Iterative maximum-likelihood sequence estimation for space-time coded systems," *IEEE Transactions on Communications*, vol. 49, no. 6, pp. 948–951, 2001.

[19] C. H. Aldana, E. de Carvalho, and J. M. Cioffi, "Channel estimation for multicarrier multiple input single output systems using the EM algorithm," *IEEE Transactions on Signal Processing*, vol. 51, no. 12, pp. 3280–3292, 2003.

[20] Y. Xie and C. N. Georghiades, "Two EM-type channel estimation algorithms for OFDM with transmitter diversity," *IEEE Transactions on Communications*, vol. 51, no. 1, pp. 106–115, 2003.

[21] C. Cozzo and B. L. Hughes, "Joint channel estimation and data detection in space-time communications," *IEEE Transactions on Communications*, vol. 51, no. 8, pp. 1266–1270, 2003.

[22] G. Stüber, *Principles of Mobile Communication*, Kluwer Academic Publishers, Dordrecht, The Netherlands, 2001.

[23] R. A. Iltis, "Joint estimation of PN code delay and multipath using the extended Kalman filter," *IEEE Transactions on Communications*, vol. 38, no. 10, pp. 1677–1685, 1990.

[24] C. Komninakis, C. Fragouli, A. H. Sayed, and R. D. Wesel, "Multi-input multi-output fading channel tracking and equalization using Kalman estimation," *IEEE Transactions on Signal Processing*, vol. 50, no. 5, pp. 1065–1076, 2002.

[25] I. Kang, M. P. Fitz, and S. B. Gelfand, "Blind estimation of multipath channel parameters: a modal analysis approach," *IEEE Transactions on Communications*, vol. 47, no. 8, pp. 1140–1150, 1999.

[26] M. C. Vanderveen, A.-J. Van der Veen, and A. Paulraj, "Estimation of multipath parameters in wireless communications," *IEEE Transactions on Signal Processing*, vol. 46, no. 3, pp. 682–690, 1998.

[27] T. Y. Al-Naffouri, "An EM-based forward-backward Kalman filter for the estimation of time-variant channels in OFDM,"

IEEE Transactions on Signal Processing, vol. 55, no. 7, pp. 3924–3930, 2007.

[28] M. K. Tsatsanis, G. B. Giannakis, and G. Zhou, "Estimation and equalization of fading channels with random coefficients," *Signal Processing*, vol. 53, no. 2-3, pp. 211–229, 1996.

[29] Y. Li, L. J. Cimini Jr., and N. R. Sollenberger, "Robust channel estimation for OFDM systems with rapid dispersive fading channels," *IEEE Transactions on Communications*, vol. 46, no. 7, pp. 902–915, 1998.

[30] T. Y. Al-Naffouri and A. Paulraj, "A forward-backward Kalman for the estimation of time-variant channels in OFDM," in *Proceedings of the 6th IEEE Workshop on Signal Processing Advances in Wireless Communications (SPAWC '05)*, pp. 670–674, New York, NY, USA, June 2005.

[31] T. Y. Al-Naffouri and N. Al-Dhahir, "A new OFDM channel estimation algorithm for high mobility scenarios," to be submitted to *IEEE Transactions on Signal Processing*.

[32] E. Larsson and P. Stoica, *Space-Time Block Coding for Wireless Communications*, Cambridge University Press, Cambridge, UK, 2003.

[33] T. Kailath, A. H. Sayed, and B. Hassibi, *Linear Estimation*, Prentice-Hall, Upper Saddle River, NJ, USA, 2000.

[34] T. Y. Al-Naffouri, A. Bahai, and A. Paulraj, "An EM-based OFDM receiver for time-variant channels," in *Proceedings of the IEEE Global Telecommunications Conference (GLOBECOM '02)*, vol. 1, pp. 589–593, Taipei, Taiwan, November 2002.

[35] S. M. Alamouti, "A simple transmit diversity technique for wireless communications," *IEEE Journal on Selected Areas in Communications*, vol. 16, no. 8, pp. 1451–1458, 1998.

[36] T. Y. Al-Naffouri, *Adaptive algorithms for wireless channel estimation: transient analysis and semi-blind design*, Ph.D. thesis, Stanford University, San Francisco, Calif, USA, January 2005.

[37] T. Y. Al-Naffouri, "Receiver design for MIMO OFDM transmission over time variant channels," in *Proceedings of the 8th IEEE Workshop on Signal Processing Advances in Wireless Communications (SPAWC '07)*, pp. 1–6, Helsinki, Finland, June 2007.

[38] T. Y. Al-Naffouri, O. Oteri, O. Awoniyi, and A. Paulraj, "Receiver design for MIMO-OFDM transmission over time variant channels," in *Proceedings of the IEEE Global Telecommunications Conference (GLOBECOM '04)*, pp. 2487–2492, Texas, USA, December 2004.

Special Issue on
Selected Papers from MultiMedia Modeling Conference 2009

Call for Papers

The 15th International Multimedia Modeling Conference (MMM2009) was held January 7–9, 2009 at EURECOM, Sophia-Antipolis, France. MMM is a leading international conference for researchers and industry practitioners to share their new ideas, original research results, and practical development experiences from all multimedia-related areas. MMM2009 is held in co-operation with the ACM Special Interest Group on MultiMedia (ACM SIGMM). This 15th edition of MMM marks the return of the conference to Europe after numerous years of activity in Asia, and we are proud to organize such a prestigious conference on the French Riviera.

MMM2009 features a comprehensive program including three keynote talks, six oral presentation sessions, three poster sessions, and one demo session. The 135 submissions included a large number of high-quality papers in multimedia content analysis, indexing, coding, as well as applications and services. We thank our 153 Technical Program Committee members and reviewers who spent many hours reviewing papers and providing valuable feedbacks to the authors. Based on the 3 or 4 (sometimes even 5) reviews per paper, the Program Chairs decided to accept only 22 as oral papers and 20 as poster papers. The acceptance rate of 32% follows the MMM tradition of accepting only the papers of the highest technical quality. Additionally, one award for the best paper was chosen.

Before submission authors should carefully read over the journal's Author Guidelines, which are located at http://www .hindawi.com/journals/ivp/guidelines.html. Prospective authors should submit an electronic copy of their complete manuscripts through the journal Manuscript Tracking System at http://mts.hindawi.com/, according to the following timetable:

Manuscript Due	May 1, 2009
First Round of Reviews	August 1, 2009
Publication Date	November 1, 2009

Lead Guest Editor

Benoit Huet, Multimedia Communications Department, EURECOM, 2229 Route des Cretes, BP 193, 06904 Sophia-Antipolis, France; benoit.huet@eurecom.fr

Guest Editors

Alan Smeaton, Centre for Sensor Web Technologies, Centre for Digital Video Processing and School of Computing, Dublin City University, Glasnevin, Dublin 9, Ireland; alan.smeaton@dcu.ie

Ketan Mayer-Patel, Department of Computer Science, University of North Carolina at Chapel Hill, Chapel Hill, NC 27599-3175, USA; kmp@cs.unc.edu

Yannis Avrithis, Image, Video and Multimedia Systems Laboratory (IVML), National Technical University of Athens, 157 73 Athens, Greece; iavr@image.ntua.gr

Special Issue on Atypical Speech

Call for Papers

Research in speech processing (e.g., speech coding, speech enhancement, speech recognition, speaker recognition, etc.) tends to concentrate on speech samples collected from normal adult talkers. Focusing only on these "typical speakers" limits the practical applications of automatic speech processing significantly. For instance, a spoken dialogue system should be able to understand any user, even if he or she is under stress or belongs to the elderly population. While there is some research effort in language and gender issues, there remains a critical need for exploring issues related to "atypical speech". We broadly define atypical speech as speech from speakers with disabilities, children's speech, speech from the elderly, speech with emotional content, speech in a musical context, and speech recorded through unique, nontraditional transducers. The focus of the issue is on voice quality issues rather than unusual talking styles.

In this call for papers, we aim to concentrate on issues related to processing of atypical speech, issues that are commonly ignored by the mainstream speech processing research. In particular, we solicit original, previously unpublished research on:

- Identification of vocal effort, stress, and emotion in speech
- Identification and classification of speech and voice disorders
- Effects of ill health on speech
- Enhancement of disordered speech
- Processing of children's speech
- Processing of speech from elderly speakers
- Song and singer identification
- Whispered, screamed, and masked speech
- Novel transduction mechanisms for speech processing
- Computer-based diagnostic and training systems for speech dysfunctions
- Practical applications

Authors should follow the EURASIP Journal on Audio, Speech, and Music Processing manuscript format described at the journal site http://www.hindawi.com/journals/asmp/. Prospective authors should submit an electronic copy of their complete manuscript through the journal Manuscript Tracking System at http://mts.hindawi.com/, according to the following timetable:

Manuscript Due	June 1, 2009
First Round of Reviews	September 1, 2009
Publication Date	December 1, 2009

Guest Editors

Georg Stemmer, Siemens AG, Corporate Technology, 80333 Munich, Germany; georg.stemmer@siemens.com

Elmar Nöth, Department of Pattern Recognition, Friedrich-Alexander University of Erlangen-Nuremberg, 91058 Erlangen, Germany; noeth@informatik.uni-erlangen.de

Vijay Parsa, National Centre for Audiology, The University of Western Ontario, London, ON, Canada N6G 1H1; parsa@nca.uwo.ca

Special Issue on
Image Processing and Analysis in Biomechanics

Call for Papers

Computational methodologies of signal processing and analysis based on 1D-4D data are commonly used in different applications in society. In particular, image processing and analysis methodologies have enjoyed increased deployment in automated recognition, human-machine interfaces, computer-aided diagnostics, robotics surgery, and biomechanics analysis.

Image processing and analysis is fundamentally a multidisciplinary area, combining elements of informatics, mathematics, statistics, psychology, mechanics and physics, among others. One of the more important applications of image processing and analysis can be found in medical imagery, which continually promotes new research and development. Present trends include using statistical or physical procedures on medical images in order to have different objectives, such as organ segmentation, shape reconstruction, motion and deformation analysis, organ registration and comparison, virtual reality, computer-assisted therapy, or biomechanic analysis and simulation.

The research related with analysis and simulation of biomechanical structures has been a source of many challenging problems, involving geometric modeling, numerical modeling, biomechanics, material models for living tissues, experimental methodologies, and mechanobiology, as well as their application in clinical environments. A critical component for true realistic biomechanical analysis and simulations is to obtain accurately, from images, the geometric data and the behavior of the desired structures. For that, the use of automatic, efficient, and robust techniques of image processing and analysis is required.

The main objective of this Special Issue on *Image Processing and Analysis in Biomechanics* is to bring together recent advances in the field. Topics of interest include, but are not limited to:

- Signal processing in biomechanical applications
- Data interpolation, registration, acquisition and compression in biomechanics
- Segmentation of objects in images for biomechanical applications
- 3D reconstruction of objects from images for biomechanical applications
- 2D/3D tracking and object analysis in images for biomechanical applications
- 3D vision in biomechanics
- Biomechanical applications involving image processing and analysis algorithms
- Virtual reality in biomechanics
- Software development for image processing and analysis in biomechanics

Before submission authors should carefully read over the journal's Author Guidelines, which are located at http://www.hindawi.com/journals/asp/guidelines.html. Authors should follow the EURASIP Journal on Advances in Signal Processing manuscript format described at the journal site http://www.hindawi.com/journals/asp/. Prospective authors should submit an electronic copy of their complete manuscript through the journal Manuscript Tracking System at http://mts.hindawi.com/, according to the following timetable:

Manuscript Due	May 1, 2009
First Round of Reviews	August 1, 2009
Publication Date	November 1, 2009

Lead Guest Editor

João Manuel R. S. Tavares, Department of Mechanical Engineering and Industrial Management, Faculty of Engineering, University of Porto, Rua Dr. Roberto Frias, 4200-465 Porto, Portugal; tavares@fe.up.pt

Guest Editor

R. M. Natal Jorge, Department of Mechanical Engineering and Industrial Management, Faculty of Engineering, University of Porto, Rua Dr. Roberto Frias, 4200-465 Porto, Portugal; rnatal@fe.up.pt